Songklanakarin J. Sci. Technol.
44 (2), 381-387, Mar. - Apr. 2022

http://www.sjst.psu.ac.th

Original Article

Physicomechanical properties of lightweight geopolymer mortar with integrated graphene nanosheets

Amun Amri[1*], Revika Wulandari[1], Selsa Idillah[1], Sunarno[1], Sulistyo Saputro[2], Harnedi Maizir[3], and Johny Wahyuadi Soedarsono[4]

[1] *Department of Chemical Engineering, Universitas Riau, Pekanbaru, Riau, 28293 Indonesia*

[2] *Department of Natural Science Education, Universitas Sebelas Maret, Surakarta, 57126 Indonesia*

[3] *Department of Civil Engineering, Sekolah Tinggi Teknologi Pekanbaru, Riau, 28293 Indonesia*

[4] *Department of Metallurgy and Material Engineering, Universitas Indonesia, Depok, 16424 Indonesia*

Received: 15 July 2021; Revised: 23 August 2021; Accepted: 16 September 2021

Abstract

Physicomechanical properties of lightweight geopolymer (LG) mortar with added graphene have been investigated. The motivation was to expand the geopolymer applications as building wall materials. LGs were prepared via pre-foaming method by mixing fly ash, fine aggregates, ordinary portland cement (OPC), alkali activator, graphene, and foam. Graphene was probed by Raman spectroscopy, while the physicomechanical properties of LGs were investigated by X-ray diffraction (XRD), Transmission Electron Microscopy (TEM), measurements of density and porosity, as well as tests of compressive strength and thermal durability. Raman spectroscopy revealed that the graphene used was graphene nanosheets (GNS) with the I_D/I_G and I_{2D}/I_G values of 0.15 and 0.4, respectively. The measured compressive strength of LG increased to around double on adding GNS up to 3 wt.%. The average density of the produced LG was 931 kg/m^3. The porosity of LG decreased around 10% with the increase of GNS content up to 3 wt.%, but the porosity of LG slightly increased on increasing the Na_2SiO_3/NaOH ratio. XRD analysis revealed that the changes in Na_2SiO_3/NaOH ratio did not change the crystal phase of LG. The addition of GNS improved the mechanical properties and thermal durability of the LG.

Keywords: physicomechanical properties, lightweight geopolymer, graphene nanosheets

1. Introduction

The construction industry is one of the fastest-growing industries today, driven by the needs of modern society (Hanif-Tahir *et al*., 2021). Along with this, the need for construction materials such as cement is also increasing sharply (Silva, Kim, Aguilar, & Nakamatsu, 2020). It is well known that the ordinary Portland cement (OPC) industry is highly energy intensive and one of the producers of greenhouse gases, which in turn harm environmental sustainability (Liu-Wu *et al*., 2020; Ranjbar, Mehrali, Alengaram, & Jumaat, 2015). For this reason, it is necessary to look for other materials that are highly mechanically durable, low-cost, as well as environmentally friendly, as alternative materials to the conventional OPC binders. Geopolymers seem to meet these criteria. Geopolymers are aluminosilicate inorganic polymer binders that form ceramic-like solids at relatively low temperatures (Liu-Wu *et al*., 2020). This material has many advantages, such as high compressive strength, high resistance to fire and acids, and it can be produced at low temperatures using abundant low-cost fly ash materials (Liu-Wu *et al*., 2020; Ranjbar *et al*., 2015).

*Corresponding author
Email address: amun.amri@eng.unri.ac.id

To date, geopolymers have not been used in the construction industry. So far, their massive use is still limited to paving blocks on roads in residential or other domestic areas (Jonbi & Fulazzaky, 2020; Petrillo, Cioffi, De Felice, Colangelo, & Borrelli, 2016; Silva *et al*., 2020). However, this application may cause soil pollution due to the leaching of the components in the geopolymer (Nath, 2020). Another promising and massive application is their potential application as building wall materials. However, for this application the density of geopolymers must be reduced to form lightweight geopolymers (LG), in order to avoid large dead weight of the building (Hanif-Tahir *et al*., 2021). This density reduction can be achieved by enriching pores in the geopolymer (Gao-Liu *et al*., 2020; Hanif-Tahir *et al*., 2021), and the porosity also improves thermal insulation properties, which leads to better conservation of energy in the buildings (Gao-Liu *et al*., 2020; Hanif-Tahir *et al*., 2021). In addition, the porous geopolymers can also be applied as adsorbents, pH buffering agents, catalysts, etc. (Novais, Pullar, & Labrincha, 2020).

Hanif-Tahir *et al*. (2021) synthesized lightweight geopolymers using natrium silicate (Na_2SiO_3) both as activator and as foam-forming material, as well as natrium bicarbonate ($NaHCO_3$) as the initial hardening agent. Although their geopolymer had suitable physicomechanical properties for lightweight concrete, both for structural and insulation purposes, the microwave oven curing system applied in this work was not economically efficient for large-scale production. Zhou and Shen (2020) studied the influence of SiO_2/Al_2O_3 ratio on the morphology and microstructure of the lightweight geopolymer. They found that the silica to alumina ratio influenced the microstructure formation, while the curing time influenced the morphology and hydration reaction. However, the hydrogen peroxide (H_2O_2) foaming agent used was quite expensive and is less suitable for large-scale lightweight geopolymer production. Wang-Zheng *et al*. (2020) reported the manufacture of lightweight geopolymer composites using an animal protein-based foaming agent with the addition of polypropylene fibers (PF) as reinforcing filler. They showed that the thermo-mechanical properties of lightweight geopolymers were strongly influenced by the amount of PF added. PF in a certain amount could also increase thermal conductivity and increase water absorption. They concluded that the PF-reinforced geopolymer had excellent thermo-mechanical properties and could also be engineered to be an environmentally friendly and durable thermal insulation material. However, the foam and the PF used in this work are considered quite expensive for large-scale production.

In this work, we investigated the physicomechanical properties of lightweight geopolymer mortar synthesized using a low-cost foam with the addition of liquid graphene nanosheets as reinforcing additive. The graphene nanosheets used were also obtained from a low-cost, facile, and green method as reported by Varrla-Paton *et al*. (2014). The liquid graphene was well dispersed in the geopolymer thus ensuring its homogeneity in the matrix. This work sought to find a breakthrough in geopolymer materials in such a way that they can be used massively as building wall materials, not only as paving blocks as is commonly found. The research results showed that the use of a low-cost conventional foam agent can produce lightweight geopolymers and the addition of graphene can maintain the high mechanical and thermal durability of the materials.

2. Materials and Methods

2.1 Preparation of LG

Materials used for LG preparation were fly ash, sodium silicate, sodium hydroxide, sand, OPC, foaming agent, graphite powder, dishwashing liquid and aquadest. Fly ash used was high calcium C-type fly ash obtained from an electrical power plant with its composition given in (Amri-Kurniawan *et al*., 2020). Sodium silicate (Na_2SiO_3) used consisted of 29.4% SiO_2, 14.7% NaO_2 and 55.9% H_2O. Sodium hydroxide (NaOH) used had purity of 99.0%. Fine aggregates (sand) used was local river sand in Riau Province Indonesia with characteristics given in (Bathara, 2013). OPC used was Portland Composite Cement (PCC) with characteristics given in (Badan Standardisasi Nasional Indonesia [BSNI], 2014). Foaming agent used was a low-cost commercial product containing active polymer ingredients. Raw graphite used was ultra-fine graphite with purity of 99.9%. Dishwashing liquid used was conventional household dishwashing liquid for daily use, widely sold in the market. This dishwashing liquid contained 19% sodium lauryl sulfate (SLS) anionic surfactant.

Fly ash was cleaned from impurities and dried at 105°C for 1h to reduce its moisture content. The graphene was synthesized using turbulence-assisted shear exfoliation (TASE) in a kitchen blender, as reported by Varrla-Paton *et al*. (2014). This method can produce a few layers in graphene with good quality, and is environmentally friendly and inexpensive. By taking 1 kg LG as the basis of mixing calculation, LGs were prepared by mixing 0.79 kg solids (79%) of fly ash, sand, and OPC (in weight proportions 4:2:1) into a media containing 0.21 kg activator solution (21%) of Na_2SiO_3 and 10 M NaOH. A 20 mg/ml dose of graphene was then added and the mixture was stirred vigorously using a hand mixer. An amount of ~ 0.01 kg of foam (10 % of weight of cement) was made by mixing foam agent and water in 1:30 %v/v proportions, and was added into the mixture and stirred again vigorously. The homogeneous paste that resulted was then poured into 10x10x10 cm^3 molds and allowed to stand for 24 hours at room temperature. The formed wet LGs were then removed from the molds and placed in an oven at 60 ºC for 24 hours. The produced LG was ready to be tested at 28 days of age. Other samples were prepared in the same way but by varying the proportions of Na_2SiO_3/NaOH (2:1; 2.5:1; and 3:1) and the amount of graphene added (0, 1, 2, 3 wt.%). The compressive strength tests had three replicates (triplo).

2.2. Characterizations

The raw graphite powder and the produced graphene were characterized using Raman spectroscopy. The vibrations of the molecules were excited using 532 nm wavelength. Measurements were performed at ten different points of each sample. The compressive strength of LGs was tested using a compressive testing machine following ASTM C579-01 (2012), ensuring that the measuring instrument had been calibrated according to the protocol. The porosity of LGs was tested following ASTM C642 (2013) where the dry-

weight, wet-weight and pseudo-weight were measured. The graphene presence in composites was probed using transmission electron microscopy (TEM) at an accelerating voltage of 120 kV. TEM sample was dispersed in absolute ethanol and dropped onto the metal grid. The mineralogical composition of LG was analyzed using XRD with Cu anode and 40 kV / 30 mA. XRD data were obtained at 25℃ in 2θ range from 5° to 100°. Thermal durability tests were carried out in furnace at temperatures of 300 - 700 ℃ for 1.5 h at atmospheric pressure. The compressive strength of LGs was compared before and after thermal treatment.

3. Results and Discussion

3.1. Raman spectra analyses

Figure 1 shows the Raman spectra of raw graphite (green line) and the produced graphene synthesized using turbulence-assisted shear exfoliation (TASE) (blue line). Generally, there are three main peaks in each spectrum, namely D band, G band, and 2D band. These peaks are the fingerprint peaks for graphite and graphene probed by Raman spectrophotometer using laser excitation of 532 nm (Childres, Jauregui, Park, Cao, & Chen, 2013; Malard, Pimenta, Dresselhaus, & Dresselhaus, 2009; Varrla-Paton *et al*., 2014). The G band and 2D band are the peaks that indicate regularity in graphite or graphene structures, whereas the D band shows irregularities or defects in graphite or graphene structures (Childres *et al*., 2013; Malard *et al*., 2009; Zhang, He, Zhang, & Chen, 2018). The peak shifts of the produced TASE graphene compared to the graphite peaks indicate success in graphite exfoliation (Childres *et al*., 2013).

The ratio of peak intensities of D and G bands (I_D/I_G) as well as the ratio of peak intensities of 2D and G bands (I_{2D}/I_G) can be used to analyze the number of graphene layers qualitatively (Zhang *et al*., 2018). From Figure 1 it can be observed that I_D/I_G for the produced graphene is 0.15 while the I_{2D}/I_G is 0.4. These are characteristic for graphene with around 5 layers or less (Zhang *et al*., 2018). The number of graphene layers can also be analyzed from the shape of the 2D peak. The more symmetrical and sharper the 2D peak shape, the fewer the number of graphene layers would be (Phiri, Gane, & Maloney, 2017). From Figure 1, the 2D band peak intensity of the produced graphene is lower than its G band, and it has a high enough symmetry without a distinct shoulder. This shape indicates graphene with 4 layers, as described by Liu, Liu, Lew, and Wang (2013) and Ni-Wang *et al*. (2007). From these elucidations, it can be concluded that the produced graphene from the TASE process in this study is graphene nanosheets (GNS) with a various numbers of layers.

The presence of the D band in the Raman spectra of the graphite and the produced TASE graphene (GNS) is due to defects in the carbon lattice edge structure (Phiri *et al*., 2017). The defect level in the structure can be observed from the D band peak intensity. High intensity of D band peak indicates a high defect rate in the structure and vice versa (Phiri *et al*., 2017). The D band peak observed in the Raman spectra of GNS in this study looks small, which means that the defect rate is small in the produced GNS. These defects are associated with the nanosheet edges, rather than with the basal plane where defects are caused by oxidation (Varrla-Paton *et al*., 2014). However, the defects do not come from the TASE process applied, but come from the graphite raw material used, which does contain D band defects as seen in Figure 1.

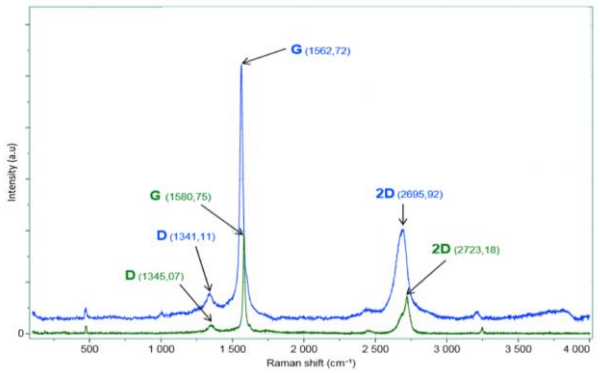

Figure 1. Raman spectra of raw graphite and the produced graphene from an exfoliation process

3.2 Compressive strength, density, and porosity of LG

Figure 2 shows the compressive strength of LG synthesized using various GNS contents and Na_2SiO_3/NaOH ratios. It can be observed that the compressive strength of LG with the addition of GNS increased significantly compared to the LG without GNS. Roughly, it increased from 1,45 MPa (compressive strength average of LG without GNS) to 2.9 MPa (compressive strength average of all LG with GNS), or around two-fold. This indicates that GNS has been well-dispersed in the geopolymer matrix and was filling the pores (Shamsaei-deSouza *et al*., 2018). Graphene or GNS has a very high specific surface area, therefore, theoretically, there is a good contact between GNS and the geopolymer matrix (Ranjbar *et al*., 2015). GNS can reduce crack expansion, fracture, and stress concentration in the geopolymer matrix due to its high modulus of elasticity, through crack deflection, crack dispersion and crack branching mechanisms (Ranjbar *et al*., 2015). The compressive strength of LG is also influenced by the ratio of Na_2SiO_3 and NaOH. The optimum compressive strength is reached at Na_2SiO_3/NaOH ratio of 2.5:1 and decreases when the ratio is increased to 3:1 (Figure 2). This could be related to the excess of sodium silicate in the geopolymer matrix, which may inhibit water evaporation and structure formation (Morsy, Alsayed, Al-Salloum, & Almusallam, 2014).

Figure 3 shows the density of LG synthesized using various GNS contents and ratios of Na_2SiO_3/NaOH. It can be noted that the average density of the produced LG was 931 kg/m^3, which is less than half the density of ordinary geopolymers (2300 kg/m^3) (Bakri-Kamarudin *et al*., 2013). Although there is one somewhat different sample, in general it can be said that an increase in the Na_2SiO_3 / NaOH ratio relatively did not significantly decrease density. This confirms that the significant decrease in compressive strength experienced by LG containing excessive sodium silicate, as indicated earlier (Figure 2), is indeed due to the inhibition of water evaporation and structure formation (Morsy *et al*., 2014) and not due to the density factor. From Figure 3 it can also be seen that increasing GNS content increased the density of LG. It can then be stated that the GNS can fill the pores or voids in

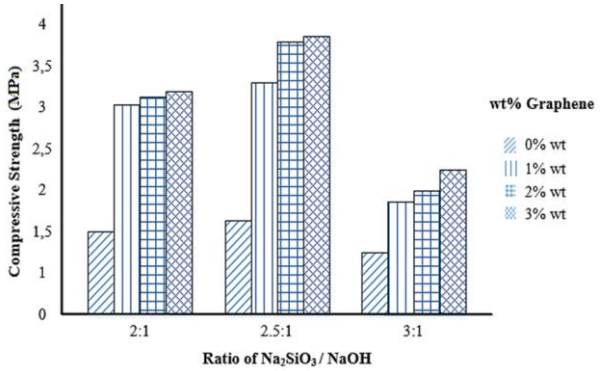

Figure 2. Compressive strength of LG synthesized with various GNS contents and activator ratios

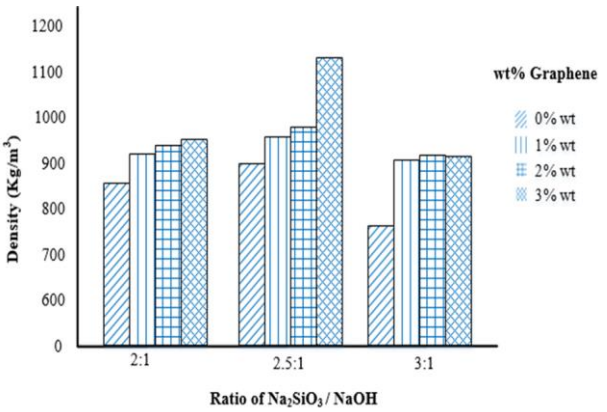

Figure 3. Density of LG synthesized using various GNS contents and activator ratios

the matrix. However, in this case, the amount of GNS added was very small, therefore its direct contribution to the density was not significant. It seems that the GNS can inhibit the rate of pore formation or pore enlargement. This notion is confirmed by Zhao-Liu *et al*. (2020), stating that graphene behaved as a template for constituents that inhibited the initial shrinkage in matrix (Zhao-Liu *et al*., 2020) leading to a reduction in pore formation. Thus, the addition of GNS also controls the strength and density of LG.

Figure 4 shows the porosity of LG synthesized using various GNS contents and ratios of Na_2SiO_3/NaOH. It can be observed that the porosity of LG decreased with GNS content. With the addition of 3% GNS, there is an average porosity decrease of around 10%, namely from 39.35% (without graphene) to 29.60% (with graphene). These results confirm the previous assumption that the addition of graphene can hold back the rate of pore formation or reduce the rate of pore enlargement. Zhao-Liu *et al*. (2020) reported that graphene behaved as template that initiated the formation of fine particles in matrix. Such a mechanism may also occur in the graphene geopolymer composite matrix, where graphene induces the formation of fine particles, which then fill the pores (Liu-Wu *et al*., 2020) decreasing porosity. From Figure 4 it can also be observed that the porosity of LG is slightly increased as the increase of Na_2SiO_3/NaOH ratio. Abdullah-Hussin *et al*. (2012) reported that a large ratio of Na_2SiO_3/NaOH in the geopolymer manufacturing will result

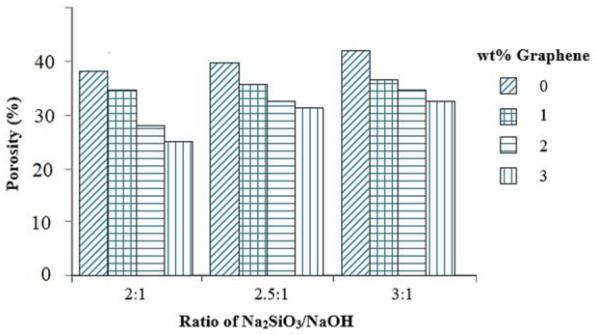

Figure 4. Porosity of LG synthesized using various GNS contents and activator ratios

in a large pore size. From this, there are opposite effects from increasing the ratio of Na_2SiO_3/NaOH and increasing the graphene content.

3.3 X-ray diffraction (XRD) and transmission electron microscopy (TEM) analyses

Figure 5 shows the XRD spectra of LG synthesized using various Na_2SiO_3/NaOH ratios and with added graphene. The LG contains minerals of Quartz (SiO_2), Mullite ($Al_6Si_2O_{13}$), Albite ($NaAlSi_3O_8$), and Maghemite (Fe_2O_3). Quartz is the most dominant peak in the spectra. This is due to the high silica (SiO_2) content. The appearance of the Albit peak indicates that the geopolymerization process has occurred forming aluminum silicate polymers in the LG matrix. The maghemite peak is from the cement used. Overall, the change in the ratio of Na_2SiO_3/NaOH in the manufacturing of LG does not change the crystal phase. The integration of graphene into LG cannot be seen clearly in this diffractogram, due to only a small amount of graphene in the composition. For this reason, verification was carried out using TEM.

Figure 6 shows TEM images of graphene in LG matrix synthesized using various Na_2SiO_3/NaOH ratios and with a 2% graphene addition. Regarding Figure 6(a-c), generally there are three parts in each figure, namely the dark part, the relatively dark part, and the transparent part. The dark part indicates a large stack of graphene layers (graphene nanoplatelet, GNP), the relatively dark part indicates a relatively large stack of graphene layers (multi-layer graphene, MLG), while the transparent part consists of a few layers of graphene (FLG), all of which can be classified as graphene nanosheets (GNS) (Childres *et al*., 2013; Ping & Fuhrer, 2012). The distributions of these three types of graphene (GNP, MLG and FLG) are relatively different from each other, which could be related to the changes in the ratio Na_2SiO_3/NaOH. The greater the Na_2SiO_3 content, the larger the portion of MLG formed compared to the portion of GNP and FLG. This is probably due to the exfoliation rate of GNP to MLG being higher than the exfoliation rate from MLG to FLG when the Na_2SiO_3 content was increased. This unique combination of GNP, MLG and FLG structures can be firmly bound in the matrix and increased the compressive strength of the matrix with synergy, as reported by Ranjbar *et al*. (Ranjbar *et al*., 2015). Overall, these TEM images also confirm that the graphene has been evenly distributed in the matrix, since the samples were taken randomly.

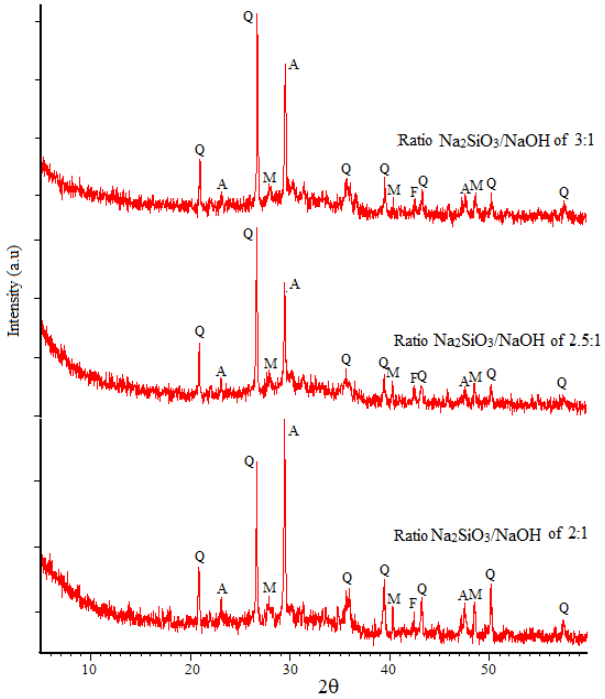

Figure 5. XRD spectra of LG synthesized using various ratios of Na2SiO3/NaOH and 2% of graphene. Q:Quartz, M:Mullite, A:Albite, and F:Maghemite

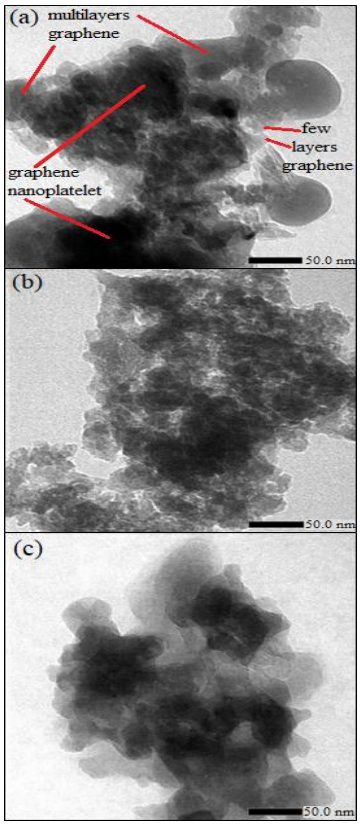

Figure 6. TEM images of samples taken from LG synthesized using 2% of graphene and Na2SiO3/NaOH ratio of (a) 2:1, (b) 2.5:1, (c) 3:1

3.4 Compressive strength of LG at high Temperature / thermal durability of LG

Figure 7 shows the compressive strength of LG after thermal durability test at various temperatures for 1.5 h. It can be seen that the compressive strength decreased significantly as the temperature was increased, but the decrease in compressive strength experienced by LG-GNS composites was not as severe as that experienced by LG without GNS. The decrease of compressive strength in LG is caused by at least two things. The first is due to the release of bound water in the chemical structure of the matrix, while the second is a dehydroxylation reaction (Zhang *et al.*, 2018). Both of these lead to the breaking of geopolymer bonds in LG and increasing pores in the matrix. The results also indicate that graphene still functions as a reinforcing material, both at low and at elevated temperatures. This can be understood, because the strength and flexibility properties of graphene do not disappear at high temperatures (Shao, Liu, Teweldebrhan, & Balandin, 2008) and it still acts as a bridge inhibiting cracks in the matrix.

The lightweight geopolymer obtained in an economical and environmentally friendly way will ensure the sustainability of production on a large scale of lightweight geopolymers as building wall materials or for other applications.

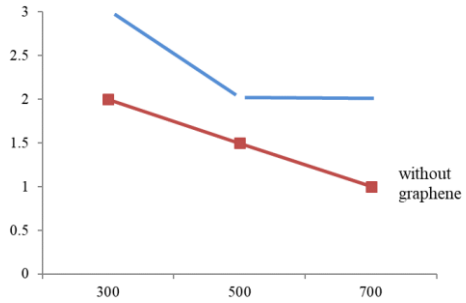

Figure 7. Compressive strength of LG synthesized using Na_2SiO_3/NaOH ratio of 2.5: 1 with and without graphene adition after thermal durability test at various temperatures for 1.5 h

4. Conclusions

Physicochemical properties of lightweight geopolymers (LG) with added graphene have been investigated. Raman spectroscopy indicated that the graphene used was graphene nanosheets (GNS). The compressive strength test results exhibited that the compressive strength of LG increased around two-fold after the addition of up to 3 wt.% GNS. The compressive strength of LG was also influenced by the ratio Na_2SiO_3/NaOH. The optimum compressive strength was reached at Na_2SiO_3/NaOH ratio of 2.5:1 and it decreased when the ratio was increased to 3:1. The density test results showed that the average density of the produced LG was 931 kg/m^3, which was less than half the density of an ordinary geopolymer. Increasing the GNS content increased the density of LG, but the increase in Na_2SiO_3/NaOH ratio relatively did not cause any significant decrease in density. The porosity test results showed that the porosity of LG decreased around 10% as the GNS content was increased to 3 wt.%, but the porosity of LG was only slightly

increased by an increased Na_2SiO_3/NaOH ratio. XRD analysis revealed that the changes in Na_2SiO_3/NaOH ratio did not change the crystal phase. TEM images confirmed the presence of GNS, which had been evenly distributed in the matrix. Thermal durability test revealed that the compressive strength of LG without GNS addition decreased significantly with thermal treatment at up to 700 ^oC, but the decrease experienced by LG-GNS composites was not as severe as that experienced by LG without GNS.

Acknowledgements

We would like to thank DIKTI for funding this research via PTUPT research grant 2021 with contract number 1369/UN.19.5.1.3/PT.01.03/2021.

References

Abdullah, M. M. A. B., Hussin, K., Bnhussain, M., Ismail, K. N., Yahya, Z., & Abdul Razak, R. (2012). Fly ash-based geopolymer lightweight concrete using foaming agent. *International Journal of Molecular Sciences*, *13*(6), 7186–7198.

Amri, A., Kurniawan, R., Sutikno, S., Yenti, S. R., Rahman, M. M., & Hendri, Y. B. (2020). Compressive Strength of Coal Fly-ash Based Geopolymer with Integration of Graphene Nanosheets (GNs). *Journal of Physics: Conference Series*, *1655*(1), 12005.

Bakri, A. M., Kamarudin, H., Binhussain, M., Nizar, I. K., Rafiza, A. R., & Zarina, Y. (2013). Comparison of geopolymer fly ash and ordinary portland cement to the strength of concrete. *Advanced Science Letters*, *19*(12), 3592–3595.

Bathara, L. (2013). Karakteristik dan potensi sedimen di Muara Sungai Kampar. *Ilmu Perairan (Aquatic Science)*, *7*(2), 11-22.

Badan Standardisasi Nasional Indonesia [BSNI]. (2014). SNI 7064-2014: Semen Portland Komposit. http://www.bbk.go.id/uploads/media/SNI_7064-2014.pdf

Childres, I., Jauregui, L. A., Park, W., Cao, H., & Chen, Y. P. (2013). Raman spectroscopy of graphene and related materials. *New Developments in Photon and Materials Research*, *1*, 1–20.

Gao, H., Liu, H., Liao, L., Mei, L., Zhang, F., Zhang, L., . . . Lv, G. (2020). A bifunctional hierarchical porous kaolinite geopolymer with good performance in thermal and sound insulation. *Construction and Building Materials*, *251*, 118888.

Hanif, S., Tahir, M. A., Rashid, K., Rehman, M. U., Saleem, N., Aslam, A., & Naeem, G. (2021). Physico-mechanical performance of lightweight geopolymer foam aggregates developed by geopolymerization through microwave-oven irradiations. *Journal of King Saud University-Engineering Sciences*.

Jonbi, J., & Fulazzaky, M. A. (2020). Modeling the water absorption and compressive strength of geopolymer paving block: An empirical approach. *Measurement*, *158*, 107695.

Liu, X., Wu, Y., Li, M., Jiang, J., Guo, L., Wang, W., . . . Duan, P. (2020). Effects of graphene oxide on microstructure and mechanical properties of graphene oxide-geopolymer composites. *Construction and Building Materials*, *247*, 118544.

Liu, Y., Liu, Z., Lew, W. S., & Wang, Q. J. (2013). Temperature dependence of the electrical transport properties in few-layer graphene interconnects. *Nanoscale Research Letters*, *8*(1), 1–7.

Malard, L. M., Pimenta, M. A., Dresselhaus, G., & Dresselhaus, M. S. (2009). Raman spectroscopy in graphene. *Physics Reports*, *473*(5–6), 51–87.

Morsy, M. S., Alsayed, S. H., Al-Salloum, Y., & Almusallam, T. (2014). Effect of sodium silicate to sodium hydroxide ratios on strength and microstructure of fly ash geopolymer binder. *Arabian Journal for Science and Engineering*, *39*(6), 4333–4339.

Nath, S. K. (2020). Fly ash and zinc slag blended geopolymer: Immobilization of hazardous materials and development of paving blocks. *Journal of Hazardous Materials*, *387*, 121673.

Ni, Z. H., Wang, H. M., Kasim, J., Fan, H. M., Yu, T., Wu, Y. H., . . . Shen, Z. X. (2007). Graphene thickness determination using reflection and contrast spectroscopy. *Nano Letters*, *7*(9), 2758–2763.

Novais, R. M., Pullar, R. C., & Labrincha, J. A. (2020). Geopolymer foams: An overview of recent advancements. *Progress in Materials Science*, *109*, 100621.

Petrillo, A., Cioffi, R., De Felice, F., Colangelo, F., & Borrelli, C. (2016). An environmental evaluation: A comparison between geopolymer and OPC concrete paving blocks manufacturing process in Italy. *Environmental Progress and Sustainable Energy*, *35*(6), 1699–1708.

Phiri, J., Gane, P., & Maloney, T. C. (2017). High-concentration shear-exfoliated colloidal dispersion of surfactant–polymer-stabilized few-layer graphene sheets. *Journal of Materials Science*, *52*(13), 8321–8337.

Ping, J., & Fuhrer, M. S. (2012). Layer number and stacking sequence imaging of few-layer graphene by transmission electron microscopy. *Nano Letters*, *12*(9), 4635–4641.

Ranjbar, N., Mehrali, M., Alengaram, U. J., & Jumaat, M. Z. (2015). Graphene nanoplatelet-fly ash-based geopolymer composites. *Cement and Concrete Research*, *76*, 222–231.

Shamsaei, E., deSouza, F. B., Yao, X., Benhelal, E., Akbari, A., & Duan, W. (2018). Graphene-based nanosheets for stronger and more durable concrete: A review. *Construction and Building Materials*, *183*, 642–660.

Shao, Q., Liu, G., Teweldebrhan, D., & Balandin, A. A. (2008). High-temperature quenching of electrical resistance in graphene interconnects. *Applied Physics Letters*, *92*(20), 202108.

Silva, G., Kim, S., Aguilar, R., & Nakamatsu, J. (2020). Natural fibers as reinforcement additives for geopolymers–A review of potential eco-friendly applications to the construction industry. *Sus tainable Materials and Technologies*, *23*, e00132.

Varrla, E., Paton, K. R., Backes, C., Harvey, A., Smith, R. J., McCauley, J., & Coleman, J. N. (2014). Turbulence-assisted shear exfoliation of graphene using household detergent and a kitchen blender. *Nanoscale*, *6*(20), 11810–11819.

Wang, Y., Zheng, T., Zheng, X., Liu, Y., Darkwa, J., & Zhou, G. (2020). Thermo-mechanical and moisture absorption properties of fly ash-based lightweight geopolymer concrete reinforced by polypropylene fibers. *Construction and Building Materials*, *251*, 118960.

Zhang, Y. J., He, P. Y., Zhang, Y. X., & Chen, H. (2018). A novel electroconductive graphene/fly ash-based geopolymer composite and its photocatalytic performance. *Chemical Engineering Journal*, *334*, 2459–2466.

Zhao, Y., Liu, Y., Shi, T., Gu, Y., Zheng, B., Zhang, K., Xu, J., Fu, Y., & Shi, S. (2020). Study of mechanical properties and early-stage deformation properties of graphene-modified cement-based materials. *Construction and Building Materials*, *257*, 119498.

Zhou, X., & Shen, J. (2020). Micromorphology and microstructure of coal fly ash and furnace bottom slag-based light-weight geopolymer. *Construction and Building Materials*, *242*, 118168.